ICIC Express Letters
Volume **14**, Number **9**, September **2020**

ICIC International ©2020 ISSN 1881-803X
pp. **891–899**

ANALYTICAL METHOD BASED ON THE ABSOLUTE NODAL COORDINATE FORMULATION FOR ELASTIC MATERIAL COMPONENTS TO REFORM THE DESIGN-STYLE OF HUMAN ASSISTIVE DEVICES

Yoshitaka Kato[1] and Hiroaki Wagatsuma[1,2,3]

[1]Graduate School of Life Science and Systems Engineering
Kyushu Institute of Technology (Kyutech)
2-4 Hibikino, Wakamatsu-ku, Kitakyushu 808-0196, Japan
kato.yoshitaka477@mail.kyutech.jp

[2]RIKEN Center for Brain Science (RIKEN CBS)
2-1 Hirosawa, Wako, Saitama 351-0198, Japan

[3]Artificial Intelligence Research Center, AIST (AIRC-AIST)
2-3-26 Aomi, Koto-ku, Tokyo 135-0064, Japan
waga@brain.kyutech.ac.jp

Received March 2020; accepted June 2020

Abstract. *In fields of soft-robotics and human assistive devices, the utilization of elastic materials is highly expected as alternatives of conventional electric actuators. On the other hand, the difficulty in combining traditional mathematical methods for rigid-body mechanics and elastic material prevents systematic and consistent analysis. In this study, we introduced the absolute nodal coordinate formulation as the extended theory and proposed the systematic evaluation of the necessary stiffness of the elastic material embedded in the human assistive devices. Our computer experiment successfully demonstrated the evaluation when the device is dynamically deforming depending on the human posture. It will contribute to opening the new era of the systematic design of human assistive devices, which will significantly reduce the trial-and-error workload of expert prosthetists.*

Keywords: Multibody dynamics, Absolute nodal coordinate formulation, Soft-robotics, Elastic materials, Human assistive devices

1. **Introduction.** As Sanchez-Villamañan et al. [1] reviewed, exoskeleton devices have been studied in the form of a rigid-body structure with compliant actuators, while recently soft exoskeletons are highlighted due to advantages in a light weight and low cost, such as Ding et al. [2] and Graf et al. [3] for assistance during walking. Interestingly, Näf et al. [4] proposed a support exoskeleton device to prevent backbone damage by using flexible beams. They practically implemented carbon-fiber beams into the spinal module of the device to help the subject to lift up the upper-body and provided a simple analysis of the stiffness and displacement based on the conventional theory of structures. However, rigid and soft exoskeletons are not alternative options and hybrid types are studied with a high expectation [1, 5]. On the other hand, theories of rigid-body mechanics and structural dynamics for elastic material such as the finite element method (called FEM) were developed individually so far, which causes the difficulty of the whole system analysis to combine rigid and soft parts together. For the sake of the solution, the absolute nodal coordinate formulation (abbreviated as "ANCF"), which was originally formulated by Shabana [6, 7], is crucial for the system evaluation of assistive devices in a comprehensive manner and enhances fair comparisons among different devices. Originally, the multibody

DOI: 10.24507/icicel.14.09.891

system dynamics (abbreviated as "MBD") [8, 9] was proposed as the systematic way to analyze rigid body mechanics. In the method, the complexity of Newton-Euler equations for all movable components was replaced in the systematic matrix formulation composed of algebraic equations from all constraints by using the single Jacobian matrix. Therefore, the theory enables complex systems to compare after the normalization of device weights and driving force conditions, as demonstrated by Komoda and Wagatsuma [10]. ANCF is an integrative theory to combine MBD and FEM to analyze any deformable material in the same systematic procedure.

In this study, we hypothesized that the ANCF facilitates the utilization of materials with a property of the elastic deformation in the aim of human assistive devices, due to an accurate estimation of the force generation depending on the human posture when it dynamically moves, with respect to the target property of the elastic material. We have proposed the carbon fiber reinforced plastic (called CFRP) beam as a component of the assistive device to provide an additional force to help human motions [11, 12]. The purpose of the present study is the establishment of the ANCF based analysis method for assistive devices with flexible beams. The paper is organized as our previous human experiments with the device with a CFRP beam in Section 2 and the basic formulation of the ANCF in Section 3. Section 4 described the comparison between results by ANCF and the conventional theory. The analysis of dynamics of the planar flexible beam in ANCF providing elastic forces during the deformation of the beam was in Section 5 and conclusions were in Section 6.

2. **Human Assistive Devices with CFRP.** In our human experiments, we investigated the effectiveness of the CFRP beam as a component to accumulate the potential energy in the standing up posture if the body is bending at the waist and then, ideally, the accumulated energy can be released in the form of a force generation when the body raises [11] (Figure 1), which is consistent with Näf et al. [4]. If the CFRP stiffness is too much hard to bend for the subject, the phenomenon cannot be used for the assistive function. Therefore, the appropriate estimation of the stiffness parameter is crucial for the realization of the function to reduce the load by the upper-body weight and associate with the muscle coordination.

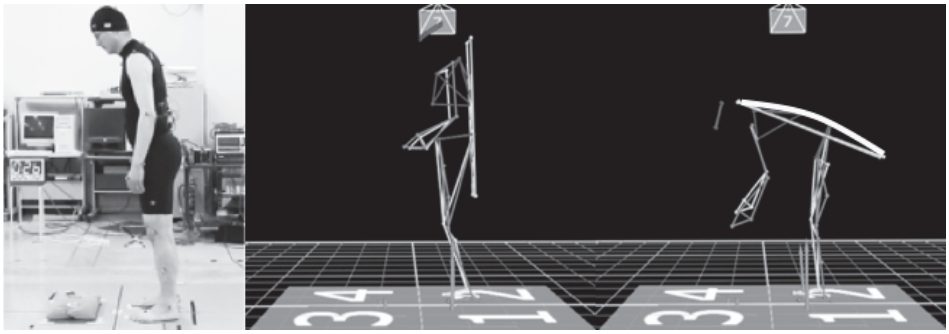

FIGURE 1. A human posture investigated with the 3D motion capture system in the experiment with CFRP to prevent a backbone problem

In the CFRP beam, the stiffness is designed by the flexural rigidity basically defined as

$$EI\frac{dy}{dx} = \int_0^x M(x)dx + C \tag{1}$$

where E is the modulus of elasticity or Young's modulus [Pa], I is the second moment of area [m^4], y is the transverse displacement of the beam at x and $M(x)$ is the bending moment at x (C is a constant). Thus, the important problem is the determination of the EI value of the CFRP beam.

3. **Theory of the Absolute Nodal Coordinate Formulation.** In following sections, mathematical formulation is described in the style of the ANCF description by Shabana [7, 9]. In the first place, the global position vector of an arbitrary point on the element can be described as

$$\mathbf{r} = \mathbf{S}\mathbf{e} \tag{2}$$

where $\mathbf{S}$ is the global shape function, and $\mathbf{e}$ is the vector of element nodal coordinates that includes global displacements and slopes defined at the nodal points of the element. The shape function can be written as

$$\mathbf{S} = \begin{bmatrix} \mathbf{S}_1 \\ \mathbf{S}_2 \end{bmatrix} = \begin{bmatrix} 1-3\xi^2+2\xi^3 & 0 \\ 0 & 1-3\xi^2+2\xi^3 \\ l\,(\xi-2\xi^2+\xi^3) & 0 \\ 0 & l\,(\xi-2\xi^2+\xi^3) \\ 3\xi^2-2\xi^3 & 0 \\ 0 & 3\xi^2-2\xi^3 \\ l\,(-\xi^2+\xi^3) & 0 \\ 0 & l\,(-\xi^2+\xi^3) \end{bmatrix}^{\mathrm{T}} \tag{3}$$

and the vector of nodal coordinates is

$$\mathbf{e} = \begin{bmatrix} e_1 & e_2 & e_3 & e_4 & e_5 & e_6 & e_7 & e_8 \end{bmatrix}^{\mathrm{T}} \tag{4}$$

where $\xi = x/l$, l is the length of the element, e_1, e_2 are global displacements of the node at A, e_5 and e_6 are global displacements of the nodes at B shown in Figure 2, and slopes are as follows.

$$e_3 = \frac{\partial r_1(x=0)}{\partial x}, \quad e_4 = \frac{\partial r_2(x=0)}{\partial x}, \quad e_7 = \frac{\partial r_1(x=l)}{\partial x}, \quad e_8 = \frac{\partial r_2(x=l)}{\partial x} \tag{5}$$

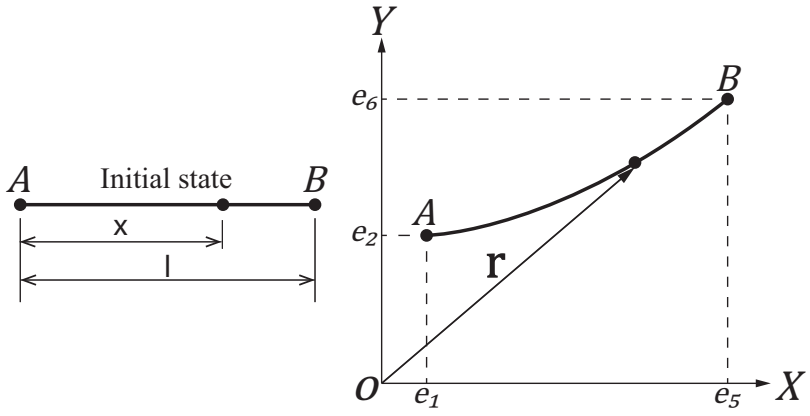

FIGURE 2. The planar beam element of ANCF

3.1. **Definition of the mass matrix.** By differentiating Equation (2) with respect to time, the absolute velocity vector can be defined. This velocity vector can be used to define the kinetic energy of the element as

$$T = \frac{1}{2}\dot{\mathbf{e}}\mathbf{M}_a\dot{\mathbf{e}} \tag{6}$$

where $\mathbf{M}_a$ is the constant mass matrix of the element defined as

$$\mathbf{M}_a = \int_V \rho \mathbf{S}^{\mathrm{T}} \mathbf{S} dV$$

$$= m \begin{bmatrix} \frac{13}{35} & 0 & \frac{11l}{210} & 0 & \frac{9}{70} & 0 & -\frac{13l}{420} & 0 \\ 0 & \frac{13}{35} & 0 & \frac{11l}{210} & 0 & \frac{9}{70} & 0 & -\frac{13l}{420} \\ \frac{11l}{210} & 0 & \frac{(l)^2}{105} & 0 & \frac{13l}{420} & 0 & -\frac{(l)^2}{140} & 0 \\ 0 & \frac{11l}{210} & 0 & \frac{(l)^2}{105} & 0 & \frac{13l}{420} & 0 & -\frac{(l)^2}{140} \\ \frac{9}{70} & 0 & \frac{13l}{420} & 0 & \frac{13}{35} & 0 & -\frac{11l}{210} & 0 \\ 0 & \frac{9}{70} & 0 & \frac{13l}{420} & 0 & \frac{13}{35} & 0 & -\frac{11l}{210} \\ -\frac{13l}{420} & 0 & -\frac{(l)^2}{140} & 0 & -\frac{11l}{210} & 0 & \frac{(l)^2}{105} & 0 \\ 0 & -\frac{13l}{420} & 0 & -\frac{(l)^2}{140} & 0 & -\frac{11l}{210} & 0 & \frac{(l)^2}{105} \end{bmatrix} \tag{7}$$

where m is the mass of the element.

3.2. **Definition of the stiffness matrices.** In this study, we used the stiffness matrices proposed by Takahashi et al. [8, 13]. The strain energy due to the longitudinal deformation can be defined as

$$U_l = \frac{1}{2} \int_0^l EA\varepsilon^2 dx \tag{8}$$

where E is the modulus of elasticity of the element, A is the cross sectional area of the element, and ε is the longitudinal strain which can be written as

$$\varepsilon = \frac{l_d - l}{l} = \frac{\sqrt{(e_5 - e_1)^2 + (e_6 - e_2)^2} - l}{l} \tag{9}$$

where $l_d \left(= \sqrt{(e_5 - e_1)^2 + (e_6 - e_2)^2} \right)$ is the length of the deformed element. Substituting Equation (9) into Equation (8) following equation can be obtained.

$$U_l = \frac{1}{2} EAl \left[\frac{1}{l^2} \left\{ (e_5 - e_1)^2 + (e_6 - e_2)^2 \right\} - \frac{2}{l} \sqrt{(e_5 - e_1)^2 + (e_6 - e_2)^2} + 1 \right] \tag{10}$$

Using Equation (10), the vector of the elastic forces in the longitudinal direction can be defined as

$$\mathbf{Q}_l = \left(\frac{\partial U_l}{\partial \mathbf{e}} \right)^{\mathrm{T}} = \mathbf{K}_l \mathbf{e} \tag{11}$$

where $\mathbf{K}_l$ is the stiffness matrix of axial strain defined as

$$\mathbf{K}_l = \frac{EA}{l} \varepsilon_d \begin{bmatrix} 1 & 0 & 0 & 0 & -1 & 0 & 0 & 0 \\ 0 & 1 & 0 & 0 & 0 & -1 & 0 & 0 \\ 0 & 0 & 0 & 0 & 0 & 0 & 0 & 0 \\ 0 & 0 & 0 & 0 & 0 & 0 & 0 & 0 \\ -1 & 0 & 0 & 0 & 1 & 0 & 0 & 0 \\ 0 & -1 & 0 & 0 & 0 & 1 & 0 & 0 \\ 0 & 0 & 0 & 0 & 0 & 0 & 0 & 0 \\ 0 & 0 & 0 & 0 & 0 & 0 & 0 & 0 \end{bmatrix} \tag{12}$$

where ε_d can be written as

$$\varepsilon_d = \frac{l_d - l}{l_d} \tag{13}$$

Note that this stiffness matrix $\mathbf{K}_l$ defined in Equation (12) must be calculated in every time step of the numerical integral because $\mathbf{K}_l$ includes the time-varying strain ε_d.

The strain energy for bending deformation can be defined as

$$U_t = \frac{1}{2}\int_0^l EI\kappa^2 dx \tag{14}$$

where κ is the radius of curvature and can be defined from geometrical relationship shown by Figure 3 as

$$\kappa = \frac{1}{\rho} = \frac{d\theta}{dx} \tag{15}$$

where ρ is the curvature radius. We assume that the extensional deformation is infinitesimal and the relation

$$\frac{\partial r_1}{\partial x} = \frac{\partial \mathbf{S}_1}{\partial x}\mathbf{e} = \cos\theta, \quad \frac{\partial r_2}{\partial x} = \frac{\partial \mathbf{S}_2}{\partial x}\mathbf{e} = \sin\theta \tag{16}$$

holds. Differentiation of preceding equations with respect to the longitudinal direction yields

$$\frac{\partial^2 \mathbf{S}_1}{dx^2}\mathbf{e} = \frac{\partial \cos\theta}{\partial x} = -\sin\theta\frac{d\theta}{dx}, \quad \frac{\partial^2 \mathbf{S}_2}{\partial x^2}\mathbf{e} = \frac{\partial \sin\theta}{\partial x} = \cos\theta\frac{d\theta}{dx} \tag{17}$$

From preceding equation, it can be found that

$$\left(\frac{\partial^2 \mathbf{S}_1}{\partial x^2}\mathbf{e}\right)^2 + \left(\frac{\partial^2 \mathbf{S}_2}{\partial x^2}\mathbf{e}\right)^2 = \left(\frac{d\theta}{dx}\right)^2 \tag{18}$$

From Equations (15) and (18), the square of κ can be obtained as

$$\kappa^2 = \left(\frac{d\theta}{dx}\right)^2 = \left(\frac{\partial^2 \mathbf{S}_1}{\partial x^2}\mathbf{e}\right)^2 + \left(\frac{\partial^2 \mathbf{S}_2}{\partial x^2}\mathbf{e}\right)^2 = \left(\frac{\partial^2 \mathbf{S}}{\partial x^2}\mathbf{e}\right)^{\mathrm{T}}\left(\frac{\partial^2 \mathbf{S}}{\partial x^2}\mathbf{e}\right) \tag{19}$$

Then Equation (14) can be rearranged as

$$U_t = \frac{1}{2}\mathbf{e}^{\mathrm{T}}\left\{\int_0^l EI\left(\frac{\partial^2 \mathbf{S}}{\partial x^2}\right)^{\mathrm{T}}\left(\frac{\partial^2 \mathbf{S}}{\partial x^2}\right)dx\right\}\mathbf{e} \tag{20}$$

Using Equation (20), the vector of the elastic forces due to the bending deformation can be defined as

$$\mathbf{Q}_t = \left(\frac{\partial U_t}{\partial \mathbf{e}}\right)^{\mathrm{T}} = \mathbf{K}_t\mathbf{e} \tag{21}$$

where $\mathbf{K}_t$ can be defined as

$$\begin{aligned}\mathbf{K}_t &= \int_0^l EI\left(\frac{\partial^2 \mathbf{S}}{\partial x^2}\right)^{\mathrm{T}}\left(\frac{\partial^2 \mathbf{S}}{\partial x^2}\right)dx \\ &= \frac{EI}{l^3}\begin{bmatrix} 12 & 0 & 6l & 0 & -12 & 0 & 6l & 0 \\ 0 & 12 & 0 & 6l & 0 & -12 & 0 & 6l \\ 6l & 0 & 4l^2 & 0 & -6l & 0 & 2l^2 & 0 \\ 0 & 6l & 0 & 4l^2 & 0 & -6l & 0 & 2l^2 \\ -12 & 0 & -6l & 0 & 12 & 0 & -6l & 0 \\ 0 & -12 & 0 & -6l & 0 & 12 & 0 & -6l \\ 6l & 0 & 2l^2 & 0 & -6l & 0 & 4l^2 & 0 \\ 0 & 6l & 0 & 2l^2 & 0 & -6l & 0 & 4l^2 \end{bmatrix}\end{aligned} \tag{22}$$

Elastic forces of the beam element due to the deformation can be obtained using Equations (11) and (21) as

$$\mathbf{Q}_k = \mathbf{Q}_l + \mathbf{Q}_t \tag{23}$$

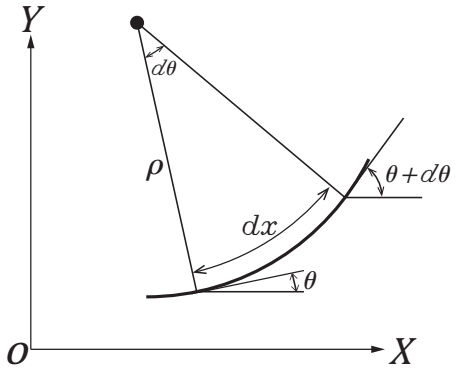

FIGURE 3. The beam element in bent state

3.3. **Definition of equations of motion.** The equation of motion of the finite element can be defined as

$$\mathbf{M}_a\ddot{\mathbf{e}} = \mathbf{Q}_a - \mathbf{Q}_k \tag{24}$$

where $\mathbf{M}_a$ is the constant mass matrix defined by Equation (7), $\ddot{\mathbf{e}}$ is the second derivative of the vector of nodal coordinates defined by Equation (4), $\mathbf{Q}_a$ is the generalized nodal forces including external forces and $\mathbf{Q}_k$ is the vector of elastic forces defined by Equation (23).

4. **Comparison of Static Theoretical Values and Calculated Values Using ANCF.** We compared the deflections of the flexible beam which has parameters of CFRP between theoretical values obtained using the following equation [14] and calculated values using ANCF (Table 1). The beam was divided into 5 elements.

$$\frac{dy^2}{dx^2} = -\frac{M}{EI} \tag{25}$$

where y is the deflection, x is the position of the longitudinal direction, M is the bending moment (Figure 4), E is the modulus of elasticity, and I is the second moment of area.

TABLE 1. Parameters of the flexible beam

Length	l	1 (m)
Modulus of elasticity	E	7.53×10^{10} (Pa)
Second moment of area	I	3.79×10^{-11} (m^4)
Density	ρ	1.5×10^3 (kg/m^3)
Bending moment	M_0	0.3 (Nm)

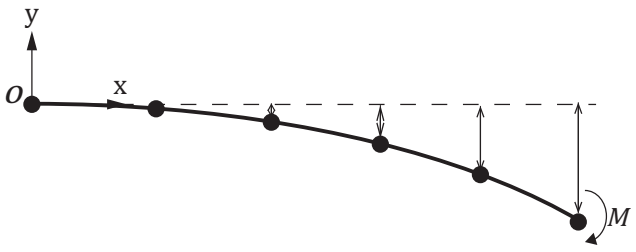

FIGURE 4. Deflections of the beam

Figure 5 shows the comparison of theoretical values obtained from Equation (25) and calculated values using ANCF. The deflections were calculated on six nodes because the beam was divided into five elements. It proved that the result of ANCF is consistent with the result from the conventional theory.

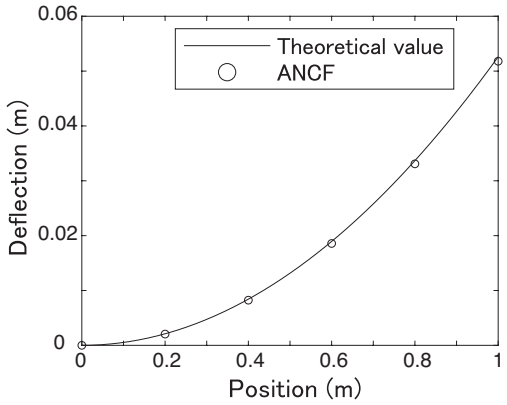

FIGURE 5. The result of the comparison of static theoretical values and calculated values using ANCF

5. **Results of Computer Experiments.** In this study, in order to evaluate the elastic force generation as an assist device, the deformation of the CFRP beam is set, which represent a bending motion, and the dynamics of the planar flexible beam to recover to the straight form was analyzed. Parameters of the beam discussed in Section 4 were shown in Table 1 except for the bending moment described in Equation (26). Figure 6(a) showed the computational model of the flexible beam in this case, which was divided into 5 elements and had 6 nodes. In the assumption, Node 1 at the bottom was fixed on the ground and the bending moment was given at Node 6 at the top of the beam as follows.

$$M(t) = \begin{cases} 1.125t \text{ Nm}, & t \leq 4.0 \\ 4.5 \text{ Nm}, & 4.0 < t \leq 4.5 \\ 0, & t > 4.5 \end{cases} \tag{26}$$

Equation (26) was given assuming that the subject wearing the assistive device bends at the waist (or the hip position) and then stops for a certain period of time and finally releases the power at the point.

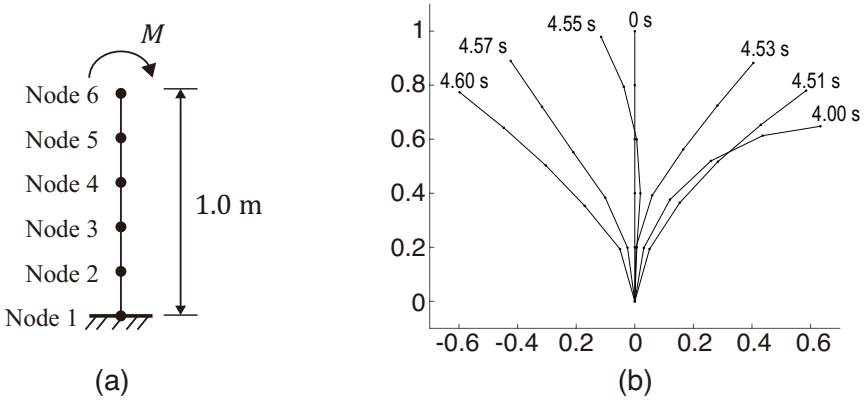

FIGURE 6. The computer experiment of the flexible beam: (a) the computational model; (b) deformed shapes of the beam

The CFRP beam was deformed with respect to the external force given at the end point (Figure 6(a)). Table 2 showed the average magnitude of elastic moments depending on individual nodes. At $t \leq 4.0$, the external force (moment) was gradually increased and then the constant bending moment was given in the time period $4.0 < t \leq 4.5$. After the period, $t > 4.5$, the beam was moving in the reversal direction to recover the original straight form. Average magnitudes of the elastic moments of Nodes 2, 3, 4 and 5 in the first and second period were mutually consistent, with respect to the difference from Nodes 1 and 6.

TABLE 2. Average magnitudes of the elastic moments depending on nodes

Time (s)	Node (Nm)					
	1	2	3	4	5	6
0-4.0	2.2908	0.0006	0.0006	0.0006	0.0006	2.2447
4.0-4.5	4.5843	0.0006	0.0006	0.0006	0.0006	4.4810
4.5-4.53062	6.3484	2.0090	1.9251	2.1164	2.6307	2.2436
4.5-5.0	5.0382	2.2731	2.0002	2.3620	2.7676	2.1269

After releasing, $4.0 < t \leq 4.5$, elastic moments at all nodes except for Node 6 increased in comparison to values in the previous periods. Interestingly, Node 1 had a high elastic moment rather than others. It represents that the elastic moment was accumulated at Node 1 after releasing from the bending shape as shown in the right side of Figure 6(b). It implies that the strain energy was stored in the beam when the external bending moment was given, and the accumulated energy at the moment was released, which acts as lifting-up force. Therefore if the CFRP beam is applied to assistive devices, the subject who wears the device receives the force generation to lift the upper-body. In addition, this result was derived when the CFRP beam is certainly fixed at the waist (or the hip position) as the ground in the computer experiment (Figure 6(a)) and it is highly important to generate the lifting force.

6. **Conclusions.** In the computer experiments, the ANCF analysis was successfully demonstrated to evaluate the force generation in the bending point. According to the assumption that the initial node is set at the waist (or the hip position) of the human-body and the end node is attached at the neck position, the lifting force can be generated from the CFRP beam and it is utilized to help the subject to raise the upper-body, which may help to prevent the backbone problem. This result implies that this method is available for the evaluation of assistive devices as how it effectively works for helping human motions. In consideration of the human body parameters such as the weight and height, the analysis reveals the effectiveness of the device at a specific time moment during a risky posture of the human body, like a backbone ache. In further analyses, this method will be combined with the human model and develop as the systematic evaluation of how much the CFRP with a special shape can generate to fit for the necessity of the human posture properly.

Acknowledgment. This work was supported in part by JSPS KAKENHI (15H05874, 16H01616, 17H06383) and the New Energy and Industrial Technology Development Organization (NEDO).

REFERENCES

[1] M. D. C. Sanchez-Villamañan, J. Gonzalez-Vargas, D. Torricelli, J. C. Moreno and J. L. Pons, Compliant lower limb exoskeletons: A comprehensive review on mechanical design principles, *Journal of NeuroEngineering and Rehabilitation*, vol.16, no.1, 2019.

[2] Y. Ding, M. Kim, S. Kuindersma and C. J. Walsh, Human-in-the-loop optimization of hip assistance with a soft exosuit during walking, *Science Robotics*, vol.3, no.15, 2018.

[3] E. S. Graf, C. Pauli, L. Erkens, G. Brinks, L. O'Sullivan, M. Wirz, M. K. S. Stadler, J. Ortiz, C. M. Bauer, V. Power, A. de Eyto, E. Bottenberg, T. Poliero, M. Sposito, D. Scherly and R. Henke, Basic functionality of a prototype wearable assistive soft exoskeleton for people with gait impairments – A case study, *The 11th ACM International Conference on PErvasive Technologies Related to Assistive Environments 2018*, pp.202-207, 2018.

[4] M. B. Näf, A. S. Koopman, S. Baltrusch, C. Rodriguez-Guerrero, B. Vanderborght and D. Lefeber, Passive back support exoskeleton improves range of motion using flexible beams, *Frontiers in Robotics and AI*, vol.5, 2018.

[5] D. Shi, W. Zhang, W. Zhang and X. Ding, A review on lower limb rehabilitation exoskeleton robots, *Chinese Journal of Mechanical Engineering*, vol.32, no.1, 2019.
[6] A. Shabana, Flexible multibody dynamics: Review of past and recent developments, *Multibody System Dynamics*, vol.1, no.2, pp.189-222, 1997.
[7] A. Shabana, Computer implementation of the absolute nodal coordinate formulation for flexible multibody dynamics, *Nonlinear Dynamics*, vol.16, no.3, pp.293-306, 1998.
[8] Y. Takahashi, Y. Terumichi and N. Shimizu, Planar dynamics analysis of flexible multibody systems, in *Multibody Dynamics (2) – Numerical Analysis and Applications*, N. Shimizu et al. (eds.), Tokyo, Corona Publishing Co., 2007 (in Japanese).
[9] A. Shabana, *Dynamics of Multibody Systems*, 4th Edition, Cambridge University Press, 2013.
[10] K. Komoda and H. Wagatsuma, Energy-efficacy comparisons and multibody dynamics analyses of legged robots with different closed-loop mechanisms, *Multibody System Dynamics*, vol.40, no.2, pp.123-153, 2017.
[11] A. Matsuda, H. Ashida, T. Saito and H. Wagatsuma, 3D morphology design of the CFRP support device for brain-body coordination prosthetics, *INCF Japan Node International Workshop: Advances in Neuroinformatics 2015 (AINI 2015)*, Tokyo, Japan, 2015.
[12] A. Matsuda, Y. Yoshida and H. Wagatsuma, A proposal of the movable fulcrum for evaluating CFRP bending shaped to fit the human body kinetics and maximize its assistive force in the aim of the orthosis design for backbone problems, *The 15th POSTECH-KYUTECH Joint Workshop on Neuroinformatics*, Pohang, Korea, 2016.
[13] Y. Takahashi and N. Shimizu, Study on the elastic force for the deformed beam by means of the absolute nodal coordinate multibody dynamics formulation. Derivation of the elastic force using finite displacement and infinitesimal strain, *Transactions of the Japan Society of Mechanical Engineers Series C*, vol.67, no.655, pp.626-632, 2001 (in Japanese).
[14] D. Chen, Bending of beam, in *Mechanics of Materials*, T. Tsuji et al. (eds.), Tokyo, The Japan Society of Mechanical Engineers, 2007 (in Japanese).